Controlling Factors of Stepwise Versus Concerted Reductive Cleavages. Illustrative Examples in the Electrochemical Reductive Breaking of Nitrogen–Halogen Bonds in Aromatic N-Halosultams

Claude P. Andrieux,[1a] Edmond Differding,[1b] Marc Robert,[1a] and Jean-Michel Savéant[1a]

Contribution from the Laboratoire d'Electrochimie Moléculaire de l'Université Denis Diderot (Paris 7) Unité Associée au CNRS No. 438, 2 place Jussieu, 75251 Paris Cedex 05, France, and Central Research Laboratories, Ciba-Geigy Ldt, CH-4002 Basel, Switzerland

Received March 8, 1993

Abstract: The cyclic voltammetry of the reductive cleavage of N-fluoro-, N-chloro-, and N-bromosaccharin sultams and of their 4-nitro-substituted analogues was investigated in acetonitrile at an inert electrode. This series of compounds provides particularly clear evidence that the two main factors governing the occurrence of a stepwise or a concerted mechanism in reductive cleavages are the energy of the π^* orbital, possibly accommodating the incoming electron, and the strength of the breaking bond. In the concerted cases, application of the theory of dissociative electron transfer allowed the estimation of the nitrogen–halogen bond dissociation energy and of the standard potential and intrinsic barrier of the reaction. The standard potential for the reduction of the nitrogen-centered sultam radicals could also be determined from the oxidation of the amide ion obtained from the reductive cleavage of the halosultams or from the deprotonation of the sultams.
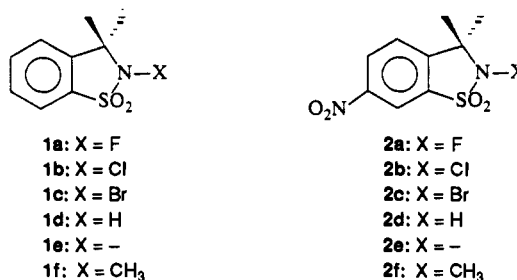
As discussed previously, the question of dissociative versus sequential mechanisms in reductive cleavages, has important

$$RX + e^- \rightleftharpoons R^\bullet + X^- \quad \text{versus} \quad RX + e^- \rightleftharpoons RX^{\bullet-} \rightarrow R^\bullet + X^-$$

implications in homogeneous and heterogeneous single electron-transfer chemistry (see refs 2a–c and references cited therein) as well as in photochemistry.[3] Previous quantitative studies in the field have concerned the cleavage of carbon–halogen bonds.[2a] With aromatic halides, electron transfer and bond breaking are stepwise in all investigated cases,[4] whereas they are concerted with simple aliphatic halides such as n-, sec-, and tert-butyl chlorides, bromides, and iodides[2a,5a] and with perfluoroalkyl halides,[2a,5b] at least in polar solvents. Benzyl and other arylmethyl halides offer the interesting example of a family of compounds within which one can pass from one mechanism to the other: with a nitro substituent the stepwise mechanism is observed, whereas for all other aryl groups, including cyanobenzyls, the concerted mechanism is followed.[6] These observations allow one to commence a systematic investigation of the structural parameters that govern the occurrence of either the concerted or the stepwise mechanism. They indeed revealed the role of the energy of the π^* orbital in which the incoming electron may be accommodated transitory: the lower the π^* orbital, the higher the probability of the stepwise mechanism to override the concerted

mechanism. Upon passing from one aryl group to the other, there is some variation of the strength of the carbon–halogen bond, but this is too small to possibly reveal its role as a factor governing the passage between stepwise and concerted mechanisms besides that of the height of the π^* orbital.

The systematic investigation of the electrochemistry of the series of aromatic sultams **1a–f** and **2a–f** that we report below was

1a: X = F	**2a:** X = F
1b: X = Cl	**2b:** X = Cl
1c: X = Br	**2c:** X = Br
1d: X = H	**2d:** X = H
1e: X = –	**2e:** X = –
1f: X = CH₃	**2f:** X = CH₃

aimed at further unraveling and illustrating the main factors that, in general, control the occurrence of one or the other mechanism. In this series of sultams, the energy of the π^* orbital is essentially varied by the introduction of the nitro substituent in the phenyl ring, whereas a substantial increase of the nitrogen–halogen bond strength is expected upon going from Br to Cl and to F, thus allowing one to test the role of this structural factor in the concerted versus stepwise mechanism dichotomy. Of particular interest in the above series of compounds is that they provide the opportunity to investigate concerted and stepwise reductive cleavages of another type of bond, the nitrogen–halogen, rather than carbon–halogen bonds as studied heretofore.

In the concerted cases, the recent extension of the Marcus–Hush model[7] of outer-sphere electron transfer to dissociative electron transfer[2a,8] will be applied to extract the dissociation energy of the nitrogen–halogen bond and the standard potential

(1) (a) Université Denis Diderot. (b) Ciba-Geigy. Present address: UCB Pharma Sector, Chemin du Foriest, B-1420 Braine-l'Alleud, Belgium.

(2) (a) Savéant, J.-M. Single Electron Transfer and Nucleophilic Substitution. In *Advances in Physical Organic Chemistry*; Bethel, D., Ed.; Academic Press: London, 1990; Vol. XXVI, pp 1–130. (b) Savéant, J.-M. Dissociative Electron Transfer. In *Advances in Electron Transfer Chemistry*; Mariano, P. S., Ed.; JAI Press: New York, in press; Vol. IV.

(3) Saeva, F. *Top. Curr. Chem.* **1990**, *156*, 61.

(4) (a) Andrieux, C. P.; Blocman, C.; Dumas-Bouchiat, J.-M.; Savéant, J.-M. *J. Am. Chem. Soc.* **1979**, *101*, 3431. (b) Andrieux, C. P.; Blocman, C.; Dumas-Bouchiat, J.-M.; M'Halla, F.; Savéant, J.-M. *J. Am. Chem. Soc.* **1980**, *102*, 3806. (c) Andrieux, C. P.; Savéant, J.-M.; Zann, D. *Nouv. J. Chim.* **1984**, *8*, 107.

(5) (a) Andrieux, C. P.; Gallardo, I.; Savéant, J.-M.; Su, K. B. *J. Am. Chem. Soc.* **1986**, *108*, 638. (b) Andrieux, C. P.; Gélis, L.; Medebielle, M.; Pinson, J.; Savéant, J.-M. *J. Am. Chem. Soc.* **1990**, *112*, 3509.

(6) Andrieux, C. P.; Le Gorande, A.; Savéant, J.-M. *J. Am. Chem. Soc.* **1992**, *114*, 6892.

(7) (a) Marcus, R. A. *J. Chem. Phys.* **1956**, *24*, 4966. (b) Hush, N. S. *J. Chem. Phys.* **1958**, *28*, 962. (c) Marcus, R. A. Theory and Applications of Electron Transfers at Electrodes and in Solution. In *Special Topics in Electrochemistry*; Rock, P. A., Ed.; Elsevier: New York, 1977; pp 161–179. (d) Marcus, R. A. *Faraday Discuss. Chem. Soc.* **1982**, *74*, 7. (e) Marcus, R. A.; Sutin, N. *Biophys. Biochim. Acta.* **1985**, *811*, 265.

and intrinsic barrier of the dissociative electron-transfer reaction. Another reason for investigating in some details[9a,b] the reductive cleavage of nitrogen–halogen bonds in *N*-halosultams is that the *N*-fluoro derivative of saccharin sultam has been shown to be an efficient and selective electrophilic fluorinating agent.[9c-e] In this connection, the discussion of the fluorination mechanism, electron transfer associated with F coupling or S_N2 substitution at the fluorine atom,[9f,g] requires a better knowledge of the mechanism of their reductive cleavage by outer-sphere electron donors.

As discussed below, the product of the electrochemical reduction of the halosultams that we investigated is the corresponding amide ion. It can also be obtained by deprotonation of the sultam itself. We thus had the opportunity to examine the oxidation of these amide ions with the aim of determining the $>N^{\bullet}/>N^{-}$ standard potential. Precise determination of amide radical/amide anion standard potentials is seldom found in the literature. It also constitutes a useful piece of knowledge in the discussion of the mechanism of the reductive cleavage of the halosultams.

Results and Discussion

Most of the cyclic voltammetric experiments were carried out at 20 °C at a glassy carbon disc electrode which appeared, among other materials, to be the best approximation of an inert electrode. As solvents we used acetonitrile and N,N'-dimethylformamide with 0.1 M n-Bu$_4$NBF$_4$ as supporting electrolyte. We did not observe any significant difference between the cyclic voltammetric behaviors in these two solvents. The results reported below are those obtained in acetonitrile.

Figure 1 shows typical cyclic voltammograms of the six *N*-halosultams at a scan rate of 0.5 V/s. Reproducibility was excellent with the two fluoro compounds but not as good with the chloro and bromo derivatives, which required careful polishing of the glassy carbon surface between each run. In the two latter cases, reproducibility was improved by decreasing the substrate concentration. The single cathodic wave in the **1** series and the first cathodic wave in the **2** series represent the two-electron irreversible reduction of the *N*-halosultam into the amide ion:

$$>N\text{--}X + 2e^- \rightarrow >N^- + X^- \qquad [1]$$
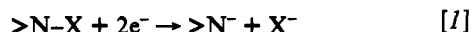
That the amide ion is the product of the reduction is attested, in the nitro-substituted series, by the fact that the one-electron reversible second wave is the same as that obtained with the nitro-substituted amide ion **2e**, generated by neutralization of the sultam **2d** by OH$^-$. This is shown in Figure 2 for **2a**. The same was observed with **2b** and **2c**.

In the nonsubstituted series, recording of the cyclic voltammogram in the presence of acetic acid shows, at very negative potentials, the appearance of a second irreversible cathodic wave identical to the wave of **1d** under the same conditions (Figure 2).

The irreversible anodic wave appearing upon scan reversal for the six halosultams represents the oxidation of the amide ion formed according to reaction *1*. It indeed has the same peak potential and irreversible characteristics whatever the halogen in each series, and these are the same as those observed upon oxidation of each amide ion generated by reaction of the sultams with OH$^-$. The fact that the anodic wave decreases when passing from Br to Cl and F merely results from the distance between the potential where the amide ion is generated and that where
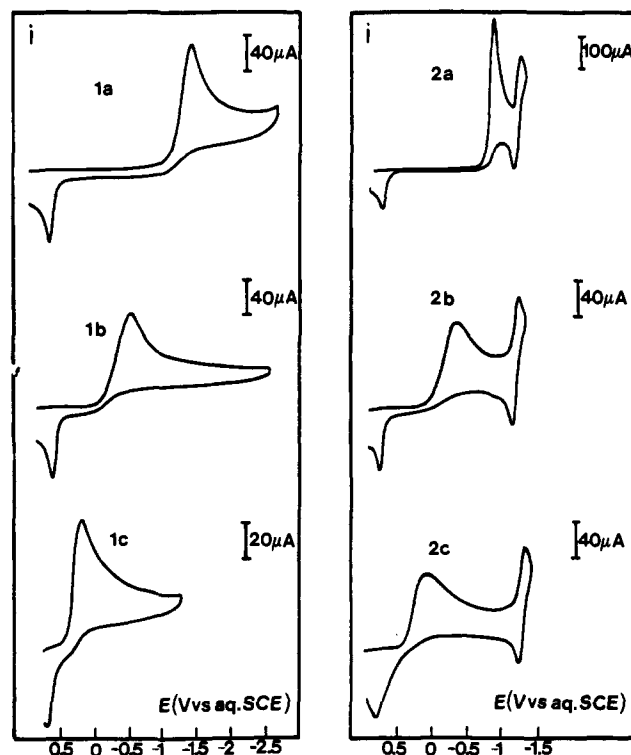

Figure 1. Cyclic voltammetry of the *N*-halosultams in acetonitrile + 0.1 M n-Bu$_4$NBF$_4$ at a glassy carbon electrode. Scan rate: 0.5 V/s. Temperature: 20 °C. Substrate concentration: 2 mM except for **2a** (4 mM).
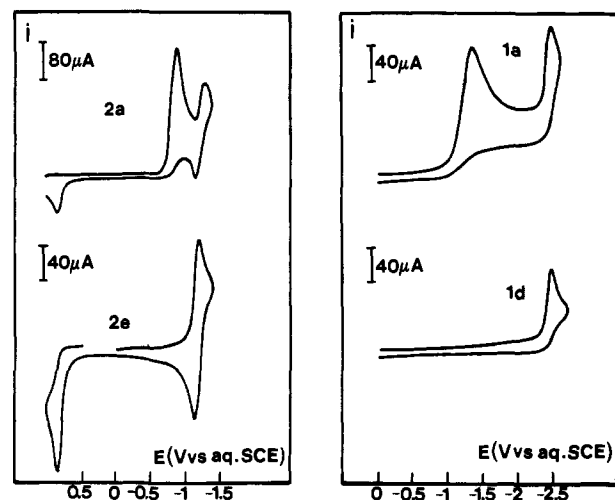

Figure 2. Cyclic voltammetry of (left) **2a** (2 mM) and **2e** (2 mM) in acetonitrile + 0.1 M n-Bu$_4$NBF$_4$ and (right) of **1d** (2 mM) and **1a** (2 mM) after addition of 2 mM CH$_3$CO$_2$H. Temperature: 20 °C. Scan rate: 1 V/s (**2a**, **2e**), 0.5 V/s (**1a**, **1d**).

it is reoxidized: more time has evolved between these two events with F than with Cl and Br, and thus more of the amide ion has diffused away from the electrode before being reoxidized.

The oxidation of the unsubstituted and nitro-substituted amide ions provides interesting pieces of information for unraveling the mechanism behind reaction *1*. Figure 3 shows the cyclic voltammograms of the amide ions **1e** and **2e** obtained from the deprotonation of the sultams **1d** and **2d** by a slightly understoichiometric amount of OH$^-$. At low scan rate (0.1 V/s), a one-electron thin ($E_{p/2}$ - E_p = 50 mV) irreversible wave is observed which tends to become reversible upon raising the scan rate. The standard potential of the $>N^{\bullet}/>N^{-}$ couple can thus be determined: 0.66 and 0.80 V vs SCE for the **1d/1e** and **2d/2e** couples,

(8) (a) Savéant, J.-M. *J. Am. Chem. Soc.* **1987**, *109*, 6788. (b) Savéant, J.-M. *J. Am. Chem. Soc.* **1992**, *114*, 10595. (c) Bertran, J.; Gallardo, I.; Moreno, M.; Savéant, J.-M. *J. Am. Chem. Soc.* **1992**, *114*, 9576.

(9) (a) The peak potential of the *N*-fluoro derivative of saccharin sultam has been reported in a preliminary account of the cyclic voltammetry of a series of similar *N*-fluoro compounds in acetonitrile.[9b] (b) Differding, E.; Bersier, P. M. *Tetrahedron* **1992**, *48* 1595. (c) Differding, E.; Lang, R. W. *Tetrahedron Lett.* **1988**, *29*, 6087. (d) Differding, E.; Lang, R. W. *Helv. Chim. Acta* **1989**, *72*, 1248. (e) Differding, E.; Rüegg, G. M.; Lang, R. W. *Tetrahedron Lett.* **1991**, *32*, 1779. (f) Differding, E.; Rüegg, G. M. *Tetrahedron Lett.* **1991**, *32*, 3815. (g) Differding, E.; Wehrli, M. *Tetrahedron Lett.* **1991**, 3819.
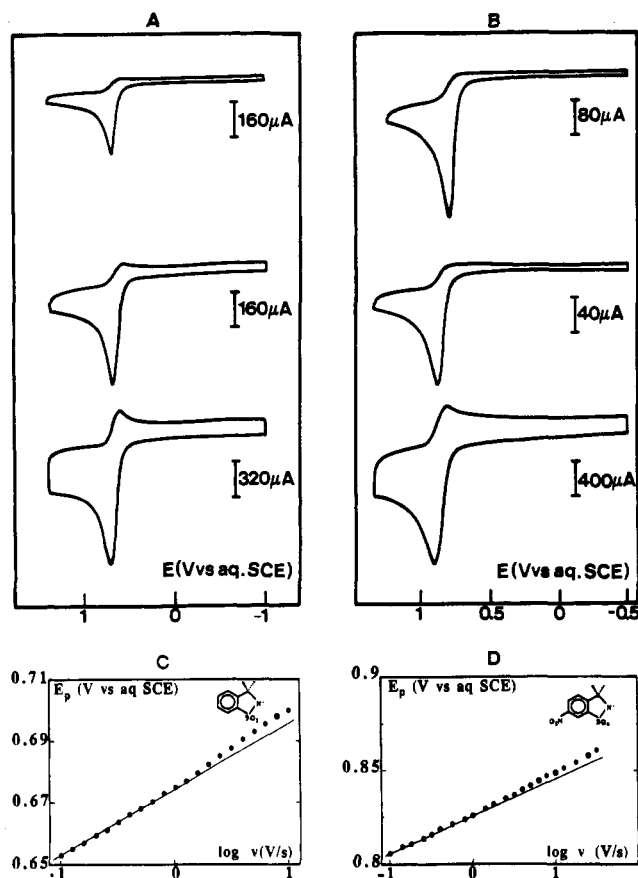
Figure 3. Cyclic voltammetry of the amide ions **1e** (A) and **2e** (B) as a function of the scan rate. Scan rate (V/s): from top to bottom, A, 2, 5, 30; B, 2, 5, 50. Diagrams C and D represent the variations of the anodic peak potential with the scan rate for **1e** and **2e**, respectively. Solvent: acetonitrile. Supporting electrolyte: 0.1 M n-Bu$_4$NBF$_4$. Temperature: 20 °C. Substrate concentration: 2 mM.

respectively. The more positive value found in the second case results from the presence of the electron-withdrawing nitro group.

The variation of the anodic peak potential with the log of the scan rate (Figure 3) is linear with a slope of 20 mV per unit between 0.1 and 1 V/s and somewhat larger above 1 V/s. This is typical of a dimerization reaction following a moderately fast electron-transfer step:[10]

$$>N^- - e^- \rightleftarrows >N^• \qquad [2]$$

$$2 >N^• \rightarrow >N-N< \qquad [3]$$

That the dimer is actually the product of the anodic oxidation was checked in the case of **1e** at the preparative scale (see Experimental Section).

These observations indicate that the two-electron reduction of the *N*-halosultams proceeds by a one-electron reduction accompanied by halide ion expulsion followed by the reduction of the ensuing >N$^•$ radical:

$$>N-X + e^- \rightarrow >N^• + X^- \qquad [4]$$

$$>N^• + e^- \rightarrow >N^- \qquad [5]$$
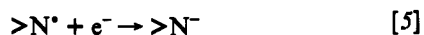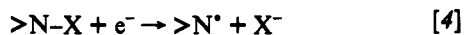
The latter reaction possesses a large driving force since its standard potential is substantially more positive than the reduction potential of the *N*-halosultams, even in the case of the bromo compounds. Approximate estimations of the standard potentials

of the X$^•$/X$^-$ couple in acetonitrile from available thermochemical data[11] lead to the following values: Br$^•$/Br$^-$, 1.48; Cl$^•$/Cl$^-$, 1.89; and F$^•$/F$^-$, 2.62 V vs aqueous SCE. There is thus in all cases a considerable thermodynamic advantage for the cleavage represented by reaction *4* against the opposite cleavage:

$$>N-X + e^- \rightarrow >N^- + X^• \qquad [6]$$
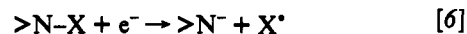
since the standard potentials of the >N$^•$/>N$^-$ couples are 0.66 and 0.80 V vs aqueous SCE in series **1** and **2**, respectively.[12] Whether or not this prediction, based on thermodynamical grounds, is modified by kinetic considerations will be discussed later on.

Another piece of helpful information for the discussion of the mechanism of reaction *4* is the estimation of the energy of the π^* orbital of the phenyl moiety of the molecule. This may be derived from the reduction characteristics of the sultams **1d, 2d** and the *N*-methylsultams **1f, 2f**.

2d and **2f** each exhibits a one-electron wave that is reversible even at scan rates as low as 0.1 V/s, corresponding to a standard potential of –0.97 and –0.95 V vs aqueous SCE, respectively.

1f shows a two-electron irreversible cathodic wave at low scan rate located at very negative potentials (the peak potential is –2.57 V vs aqueous SCE at 1 V/s). No reoxidation wave appears before 1 V vs aqueous SCE, showing that the amide ion is not formed upon reduction. The cathodic wave tends to become reversible upon raising the scan rate and the electron stoichiometry to decrease toward 1 e/molecule. The ensuing standard potential is –2.56 V vs aqueous SCE. The reduction of **1d** exhibits a quite different behavior: in the absence of added acid it shows a negative one-electron irreversible cathodic wave (peak potential: –2.50 V vs aqueous SCE at 1 V/s) which shows no tendency to become reversible up to 2000 V/s. There is a reoxidation wave that has exactly the same characteristics as that of **1e**. The variation of the cathodic peak potential with the log of the scan rate is linear with a slope of 30 mV per unit, indicating that the reaction is kinetically controlled by a first-order chemical step following a fast electron transfer.[10] Upon addition of an acid such as acetic acid, the wave becomes catalytic. This set of observations suggests the following reduction scheme:

$$>NH + e^- \rightarrow >NH^{•-} \qquad [7]$$

$$>NH^{•-} \rightarrow >N^- + {}^1/_2H_2 \qquad [8]$$
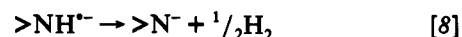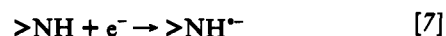
followed, in the presence of an acid (AH), by

$$>N^- + AH \rightarrow >NH + A^- \qquad [9]$$
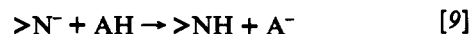
We now come to the central mechanistic question of the present discussion: is the one-electron reductive cleavage represented by reaction *4* an elementary step or the succession of two successive steps implying the intermediacy of the anion radical, as in:

$$>N-X + e^- \rightleftarrows >N-X^{•-} \qquad [10]$$

$$>N-X^{•-} \rightarrow >N^• + X^- \qquad [11]$$
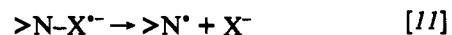
Examination of the cyclic voltammograms in Figure 1 reveals a striking difference between the reductive behavior of **2a** and that of all five other *N*-halosultams. The latter all exhibit a broad wave, characteristic of a reaction kinetically controlled by

(10) Andrieux, C. P.; Savéant, J.-M. *Electrochemical Reactions*. In *Investigation of Rates and Mechanisms of Reactions, Techniques of Chemistry*; Bernasconi, C. F., Ed.; Wiley: New York, 1986; Vol. VI/4E, Part 2, pp 305–390.

(11) (a) *Handbook of Chemistry and Physics*, 72nd ed.; CRC: Cleveland, OH, 1991–1992; p 5–1. (b) Pearsons, R. C. *J. Am. Chem. Soc.* **1986**, *108*, 6109. (c) Wagman, D. D.; Evans, W. H.; Parker, V. B.; Schumm, R. H.; Halow, I.; Bailey, S. M.; Churney, K. L.; Nuttall, R. L. *J. Phys. Chem. Ref. Data* 2–1. Suppl. 2, **1982**, *11*. (d) Marcus, Y. *Pure Appl. Chem.* **1985**, *51*, 1103.

(12) (a) The situation is different in the case of *N*-bromosuccinimide where cleavage reaction *8* is predicted to prevail on thermodynamical grounds as actually observed experimentally in pulse radiolysis.[12b] Although hypothesized, clear-cut evidence for the intermediacy of the anion radical in electrochemical or pulse radiolysis is lacking.[12b] (b) Lind, J.; Shen, X.; Eriksen, T. E.; Merenyi, E.; Eberson, L. *J. Am. Chem. Soc.* **1991**, *113*, 4929.
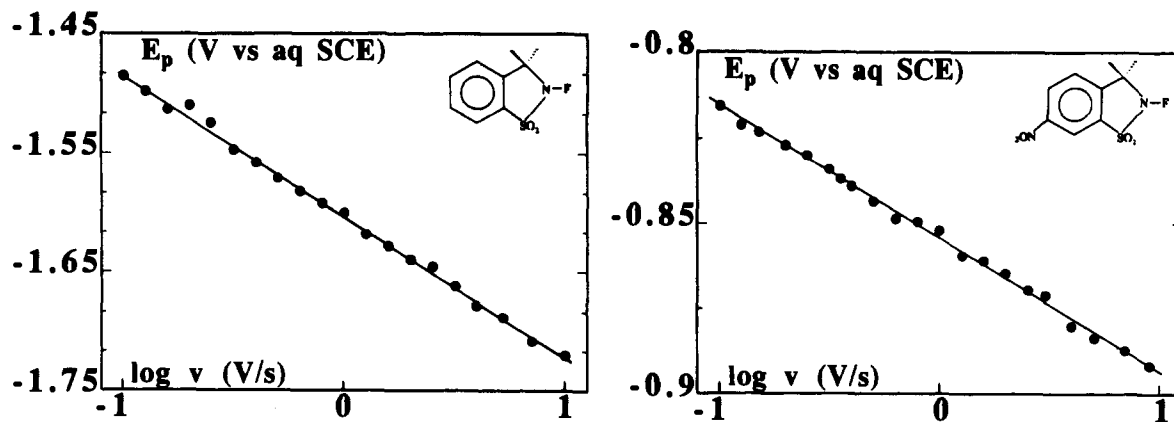
Figure 4. Variations of the cathodic cyclic voltammetric peak potentials of **1a** and **2a** with the scan rate. Reactant concentration: 2 mM. Solvent: acetonitrile. Supporting electrolyte: 0.1 M n-Bu$_4$NBF$_4$. Temperature: 20 °C.
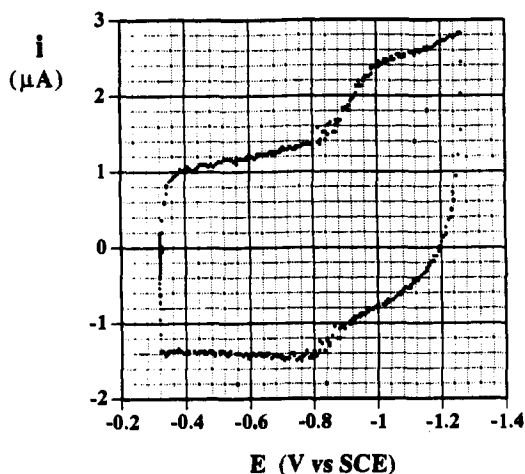

Figure 5. High-scan-rate cyclic voltammetry (47 600 V/s) of **2a** (6.1 mM) in acetonitrile + 0.6 M Et$_4$NBF$_4$ at a 10-μm carbon disc electrode. Temperature: 25 °C.

an irreversible electron-transfer step[10] with a small transfer coefficient (α) ranging from 0.2 to 0.4 as derived from the values of the peak width, $E_{p/2} - E_p$.[13a] In contrast, **2a** gives rise to a much thinner peak ($E_{p/2} - E_p$ = 58, 70, and 80 mV at 0.1, 1, and 10 V/s, respectively) pointing to a mixed kinetic control by an electron- transfer step followed by a fast homogeneous reaction.[10] This is confirmed by the variations of the peak potential with the scan rate that are represented in Figure 4. The slope of the linear plot, 39.5 mV per unit, also indicates a mixed electron-transfer follow-up homogeneous reaction rate control.[10] In the case of **1a**, the E_p vs log v plot has a slope of 127 mV per unit, confirming an irreversible electron-transfer rate control with a small transfer coefficient (α = 0.25).[13b]

All the cyclic voltammetric characteristics observed with **2a** thus point to a two-step process in which the first electron uptake [10] is followed by the rapid cleavage of the N–F bond [11]. This conclusion is further confirmed by the results of a fast-scan-rate investigation of the reduction of **2a** at a carbon ultramicroelectrode.[14] Reversibility of the wave begins to appear at 35 000 V/s and increases up to 47 000 V/s (Figure 5), the maximal value we could reach, thus allowing the estimation of **2a/2a**$^{\cdot-}$ standard potential (−0.89 V vs aqueous SCE). It is interesting to note that the value thus found is close to that obtained with the corresponding sultam **2d** and the N-methylsultam **2f**, showing that the

(13) (a) E_p = peak potential; $E_{p/2}$ = half-peak potential:

$$\alpha \approx \frac{RT}{F} \frac{1.85}{E_{p/2} - E_p}$$

(b) $\partial E_p / \partial \log v$ = −29.5/α at 20 °C.
(14) Andrieux, C. P.; Hapiot, P.; Savéant, J.-M. *Chem. Rev.* **1990**, *90*, 723.

height of the π^* orbital is not dramatically affected by the nature of the group bound to the nitrogen. The reversible peak of the amide ion **2e** is only slightly more negative ($E°$ = −1.16 V vs aqueous SCE). Therefore, the small distance separating the first (irreversible) peak from the second (reversible) peak of **2a** at low scan rate (Figure 1) constitutes by itself a clue of the stepwise character of the reductive cleavage in this case.

All the five other halosultams are characterized by a small value of the symmetry factor (transfer coefficient) α (see Table I). If one assumes that the activation–driving force law is quadratic,

$$\Delta G^{\ddagger} = \Delta G_0^{\ddagger}\left(1 + \frac{\Delta G°}{4\Delta G_0^{\ddagger}}\right)^2 \tag{1}$$

($\Delta G^{\ddagger}$, activation free energy; intrinsic barrier free energy; $\Delta G°$, free energy of the reaction), as predicted for both outer-sphere[7] and dissociative electron transfer,[2,8] a value of the symmetry factor

$$\alpha = \frac{\partial \Delta G^{\ddagger}}{\partial \Delta G°} = \frac{1}{2}\left(1 + \frac{\Delta G°}{4\Delta G_0^{\ddagger}}\right) \tag{2}$$

significantly smaller than 0.5 indicates that the driving force is large, i.e., that the standard potential of the controlling reaction is much positive to the potential at which the reduction is actually observed, here the peak potential. This condition is not achieved for the outer-sphere electron-transfer reaction *10* since the corresponding standard potential, being located in the same region as those of the corresponding >N–H/>N–H$^{\cdot-}$ and>N–CH$_3$/ >N–CH$_3$$^{\cdot-}$ couples, not only is not positive to the peak potential but is in fact much negative to it.

The large distance between the reduction potential and the expected standard potential for the >N–X/>N–X$^{\cdot-}$ reaction (**1a**, 1.07; **1b**, 2.15; **1c**, 2.71; **2b**, 0.72; and **2c**, 1.14 V at 0.1 V/s) is by itself, regardless of the small value of α, a clear indication that the stepwise mechanism is inoperative: even if the follow-up cleavage reaction *11* were very fast, the wave could not, starting from the reversible >N–X/>N–X$^{\cdot-}$ potential, shift positively by such a large amount because kinetic control by forward reaction *10* would take over much before such a positive potential could be reached (for a more detailed discussion of this point see ref 6).

We are thus led to conclude that the reductions of **1a**, **1b**, **1c**, **2b**, and **2c** are dissociative electron-transfer reactions in which the electron-transfer and bond-breaking steps are concerted.

We may then use the dissociative electron-transfer theory[2,8] to estimate the homolytic dissociation energy D_{NX} of the N–X bonds. In this purpose we employed the same strategy recently applied to benzyl and other arylmethyl halides.[6,8b] The key equations in

Table I. Determination of N–X Bond Dissociation Energies, Standard Potentials, and Intrinsic Barrier Free Energies from the Peak Potentials of the *N*-Halosultams Undergoing Dissociative Electron Transfer[a]

compd	scan rate (V/s)	$-E_p$ (V/SCE)	$-\phi_r$ (mV)	$a_X, a_{RX},$ $a(\text{Å})$	$A \times 10^{-4}$ (cm/s), λ_0, C (eV)	ΔG^* (meV)	D (eV)	$-E^\circ,$ (V/SCE)	$\Delta G_0^*,$ (meV)	α_{theor}	α_{exptl}
1a	0.1	1.49	70	1.33	4.2	392	2.82	0.14	1025	0.31	0.30
	1	1.60	71	2.25	1.28	363	2.86	0.10	1035	0.30	0.28
	10	1.72	73	2.46	2.96	335	2.84	0.12	1030	0.29	0.28
							av = 2.84	av = 0.12	av = 1030		
1b	0.1	0.41	17	1.81	4.1	389	1.89	0.44	750	0.36	0.22
	1	0.53	33	4.38	1.10	360	1.90	0.43	750	0.35	0.20
	10	0.68	41	2.87	2.33	332	1.94	0.39	760	0.33	0.18
							av = 1.91	av = 0.42	av = 750		
1c	0.1	−0.20	−43	1.96	3.7	385	1.17	0.54	550	0.42	0.42
	1	−0.17	−39	4.23	1.05	356	1.15	0.56	550	0.40	0.40
	10	−0.13	−38	3.01	1.705	328	1.13	0.58	550	0.39	0.39
							av = 1.15	av = 0.56	av = 550		
2b	0.1	0.14	−17	1.81	3.8	387	1.75	0.58	710	0.37	0.27
	1	0.26	0	4.55	1.09	358	1.76	0.57	710	0.36	0.25
	10	0.38	18	2.90	2.33	330	1.77	0.56	720	0.34	0.20
							av = 1.76	av = 0.57	av = 710		
2c	0.1	−0.35	−48	1.96	3.5	383	1.08	0.63	530	0.42	0.41
	1	−0.32	−47	4.22	1.05	354	1.05	0.66	530	0.41	0.38
	10	−0.21	−43	3.01	1.705	326	1.08	0.63	530	0.39	0.35
							av = 1.07	av = 0.65	av = 530		

[a] In CH_3CN + 0.1 M n-Bu_4NBF_4, 20 °C. Substrate concentration (mM): **1a** and **1b**, 2.0; **1c**, 0.5; **2b**, 1.0; **2c**, 0.3.

this derivation are the following. The activation free energy at the peak potential is given by

$$\Delta G^{\ddagger} = \frac{RT}{F} \ln\left[A\left(\frac{RT}{\alpha F v D}\right)^{1/2} \right] - 0.78\frac{RT}{F} \qquad (3)$$

(Where A is the preexponential factor, D the diffusion coefficient, v the scan rate, and α the transfer coefficient)

$$\Delta G^{\ddagger} = \Delta G_0^{\ddagger}\left(1 + \frac{E_p - E^\circ_{NX/N\cdot+X^-} - \phi_R}{4\Delta G_0^{\ddagger}}\right)^2 \qquad (4)$$

with

$$\Delta G_0^{\ddagger} = \frac{D_{NX} + \lambda_0}{4} \qquad (5)$$

($\Delta G_0^{\ddagger}$, intrinsic barrier free energy; λ_0, solvent reorganization factor; E_p, peak potential; ϕ_r, potential at the reaction site).

On the other hand, the standard potential may be related to the bond dissociation energy according to

$$E^\circ_{NX/N\cdot+X^-} = -D_{NX} + E^\circ_{X\cdot/X^-} - T(\bar{S}_{NX} - \bar{S}_{N\cdot} - \bar{S}_{X\cdot}) \qquad (6)$$

where the $\bar{S}$ values are the partial molar entropies of the subscript species. For the same halogen,

$$C = E^\circ_{X\cdot/X^-} - T(\bar{S}_{NX} - \bar{S}_{N\cdot} - \bar{S}_{X\cdot}) \qquad (7)$$

is about constant whatever the exact structure of the molecule. Thus:

$$D_{NX} = \frac{1}{2}\{[(\lambda_0 + E_p - C - \phi_r - \Delta G^{\ddagger})^2 + 4\lambda_0\Delta G^{\ddagger} - (\lambda_0 + E_p - C - \phi_r)^2]^{1/2} - (\lambda_0 + E_p - C - \phi_r - \Delta G^{\ddagger})\} \qquad (8)$$

A and λ_0 were estimated by comparison with data pertaining to the outer-sphere electron transfer to aromatic hydrocarbons as described in refs 6 and 8b. The estimation of λ_0 requires three equivalent sphere radii: a_X for the halogen, a_{NX} for the remainder of the molecule, and $a = a_X(2a_{NX} - a_X)/a_{NX}$. C was taken as equal to the values pertaining to $PhCH_2Br$, $PhCH_2Cl$, and $PhCH_2F$, which are themselves obtained from available thermochemical data.[11] The values of the various parameters thus used are listed in Table I together with the ensuing values of D_{NX} derived from eq 8. The table also lists the values of the standard

potential $E^\circ_{NX/N\cdot+X^-}$ and of the intrinsic barrier free energy derived from eqs 6 and 5, respectively.

The transfer coefficient predicted by the above theoretical analysis,

$$\alpha_{pred} = \frac{1}{2}\left(1 + \frac{E_p - E^\circ_{NX/N\cdot+X^-} - \phi_r}{4\Delta G_0^{\ddagger}}\right) \qquad (9)$$

may be compared with the values derived from the peak width experimental data.[13a] It is seen that a good agreement is found in most cases, including the predicted variation of α with the driving force, which appears here under the form of a variation with the scan rate.[15]

As discussed before,[6] if one neglects the quadratic character of eq 4, the variations of the bond dissociation energies may straightforwardly be related to the variations of the peak potentials at the same scan rate keeping the halogen constant by

$$D_{ZX} = -\frac{2}{3}E_p + \text{constant} \qquad (10)$$

(Z: C, N, or other atoms).

This relationship may be generalized to the case where the leaving group does not remain the same. Then,

$$D_{ZX} = -\frac{2}{3}(E_p - E^\circ_{X\cdot/X^-}) + \text{constant} \qquad (11)$$

Figure 6 shows that this relationship provides a satisfactory description of the variations of the bond dissociation energy with the peak potential in a broad series of compounds including, besides the present *N*-halosultams, aliphatic and arylmethyl halides, the bond dissociation energy of a part of which could be obtained from available thermochemical data.

The N–X bond dissociation energy is not much affected by the presence of the nitro substituent. It slightly decreases upon introduction of the nitro substituent, going in the same direction as already observed in the case of benzyl halides with electron-withdrawing groups.[6] Its values in the unsubstituted case, 2.9,

(15) (a) The peak potential E_p shifts negatively upon raising the scan rate and therefore makes $\Delta G^\circ = E_p - E^\circ_{NX/N\cdot+X^-} - \Phi_r$ more and more negative, i.e., the driving force larger. (b) There is a general trend, unexplained for the moment, for the experimental values of α to be smaller than the predicted values; the more so the larger the scan rate. This is particularly true for the two chloro compounds for which the peak location and width appeared to be the most critically dependent upon the polishing of the electrode surface.
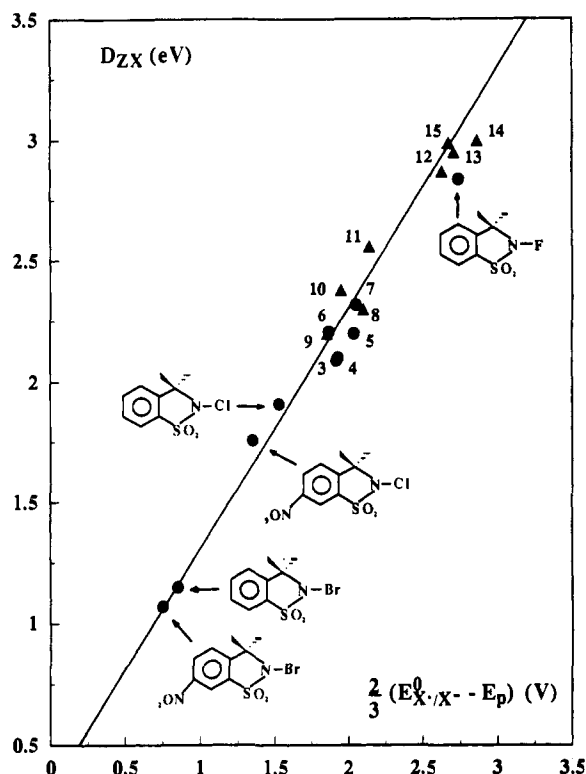
Control of Stepwise vs Concerted Reductive Cleavages

J. Am. Chem. Soc., Vol. 115, No. 15, 1993 6597

Figure 6. Correlation between bond dissociation energies and reduction peak potentials (at 0.1 V/s). ▲: D_{ZX} derived from thermochemical data. ●: D_{ZX} derived from eq 8. The straight line features eq 11 ($E^{\bullet}_{X_{\cdot}/X^{-}}$ = 0.89, 1.48, 1.89, 2.62 V vs aqueous SCE for I, Br, Cl, F, respectively). Halides at the numbered points are as follows: 3, 2-cyanobenzyl bromide; 4, 4-cyanobenzyl bromide; 5, 3-cyanobenzyl bromide; 6, 4-carbomethoxybenzyl bromide, 7, 9-anthracenylmethyl chloride; 8, benzyl bromide; 9, *tert*-butyl iodide; 10, *sec*-butyl iodide; 11, *n*-butyl iodide; 12, *tert*-butyl bromide; 13, *sec*-butyl bromide; 14, *n*-butyl bromide; 15, benzyl chloride.

1.9, and 1.2 eV for F, Cl, and Br, respectively, are, as expected, much smaller than for typical corresponding carbon–halogen bonds (4.7, 3.7, and 3.0 eV for CH_3F, CH_3Cl, and CH_3Br, respectively[16]).

We may now rationalize the factors that govern the reductive cleavage mechanism. One is the energy of the π^* orbital that may accommodate the incoming electron. The role of this factor is clearly apparent in the comparison between **1a**, which undergoes a concerted reductive cleavage, and **2a**, where the anion radical appears as an intermediate on the reaction pathway. The energy of the π^* orbital is 1.6 eV higher in **1a** than in **2a**, as estimated from the standard potential difference between **1f** and **2f**, whereas the N–F bond dissociation energy is about the same in both cases. We thus confirm the role of this factor already revealed by the previous study of the reductive cleavage of arylmethyl halides.[6]

A second essential governing factor that is revealed by the present study is the strength of the cleaving bond. The reason that **2b** cleavage is of the concerted type whereas that of **2a** is of the stepwise type derives from the large difference in the bond dissociation energy of the order of 1 eV (the bond dissociation energy of **2a** may be taken as approximately equal to that of **1a**), whereas the π^* orbital energies are about the same. The role of this factor also clearly appears when comparing **2b** and **2c**, which both undergo a concerted reductive cleavage to the nitro-substituted benzyl chlorides and bromides which follows a stepwise mechanism: the bond dissociation energy is *ca.* 1 eV less in the first case than in the second.
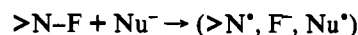
The role thus revealed of the bond dissociation energy in governing the passage from the stepwise to the concerted

mechanism now allows one to understand the sharp difference in behavior between aryl and arylmethyl halides bearing the same halogen and the same aryl group. Whereas the stepwise mechanism is followed in the first case regardless of the aryl moiety, it is only observed with nitro substituents in the second case. The essential reason for this difference is that the bond dissociation energy is again *ca.* 1 eV higher in the first case than in the second at constant or about constant π^* orbital energy.

The values of $E^{\circ}_{NX/N^{\bullet}+X^-}$ and of the intrinsic barrier $\Delta G_0^{\ddagger}$ found for **1a** (Table I) may be used to discuss the nature of the mechanism, dissociative electron transfer followed by radical coupling or S_N2 at the fluorine atom, of the fluoration of nucleophiles by this compound.[2g] A first point consists in examining the reaction of **1a** with N,N'-tetramethylphenylene-diamine in acetonitrile at 22 °C where no fluorination occurs, and that can consequently be taken as a prototype of a reaction taking place by simple dissociative electron transfer. From the intrinsic characteristics of the oxidation of this compound into its cation radical (E° = 0.00 V vs aqueous SCE[17a] and λ = 0.45 eV[17b]) and those of **1a** (Table I), the predicted value of the rate constant is 2×10^{-5} M^{-1} s^{-1} (the preexponential factor is taken as equal to 5.1×10^{12} M^{-1} s^{-1} [8b]) without taking account of the free energy of formation of the successor complex. This results from the attractive electrostatic interaction between the N,N'-tetramethylphenylenediamine cation radical and the fluoride ion. Comparison between the predicted and the experimental values of the rate constant (10^{-3} M^{-1} s^{-1} [2g]) indicates that the free energy of the interaction would be *ca.* 0.2 eV, which does not seem unreasonable in view of the small size of F^- and the likely localization of the positive charge on one of the nitrogen of the cation radical in the successor complex ion pair.

For the other electron donors that have been reacted with **1a**, there are more uncertainties on the estimation of their standard potentials and intrinsic reorganization energies. Solvents other than acetonitrile have been used, and temperature was often much below room temperature. However, the fact that for nucleophiles that effectively undergo fluorination, the predicted rate constants for dissociative electron transfer are very much below the experimental rate constants (Table II), leaves little doubt that the reaction then takes place according to an S_N2 mechanism at fluorine rather than a dissociative electron-transfer mechanism.

The fact that fluorination by **1a** does not proceed by an electron-transfer mechanism may be explained as follows. In the solvent cage where the various species resulting from dissociative electron transfer are present immediately after the reaction

$$>N-F + Nu^- \rightarrow (>N^{\bullet}, F^-, Nu^{\bullet})$$

formation of FNu by coupling between $F^{\bullet}$ and $Nu^{\bullet}$ would have required the generation of $>N^-, F^{\bullet}$ rather than $>N^{\bullet}$, F^-, against a huge driving force disadvantage (1.96 eV).

A last outcome of the present study is the experimental determination of the standard potential of the $>N^{\bullet}/>N^-$ couples. While data on the reduction of alkyl radicals are currently becoming available,[18–20] no such data have so far appeared for nitrogen-centered radicals. An interesting observation is the substantial positive shift of the standard potential (from 0.66 to 0.8 V vs aqueous SCE) triggered by the introduction of a nitro substituent in the phenyl ring, showing that this electron-

(17) (a) Eberson, L. *Electron Transfer Reactions in Organic Chemistry*; Springer Verlag: Berlin, 1987. (b) Grampp, G.; Jänicke, W. *Ber. Bunsen Ges. Phys. Chem.* **1991**, *95*, 904.
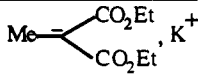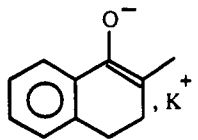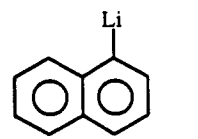
(18) (a) Wayner, D. D. M.; Griller, D. *J. Am. Chem. Soc.* **1985**, *107*, 7764. (b) Sim, B. A.; Griller, D.; Wayner, D. D. M. *J. Am. Chem. Soc.* **1989**, *111*, 754. (c) Griller, D.; Martino Simoes, J. A.; Mulder, P.; Sim, B. A.; Wayner, D. D. M. *J. Am. Chem. Soc.* **1989**, *111*, 7832. (d) Sim, B. A.; Milne, P. H.; Griller, D.; Wayner, D. D. M. *J. Am. Chem. Soc.* **1990**, *112*, 6635.

(19) Andrieux, C. P.; Gallardo, I.; Savéant, J.-M. *J. Am. Chem. Soc.* **1989**, *111*, 1620.

(20) Occhialini, D.; Kristensen, J.-S.; Daasberg, K.; Lund, H. *Acta Chem. Scand.* **1992**, *46*, 474.

(16) *Handbook of Chemistry and Physics*, 72nd ed.; CRC: Cleveland, OH 1991–1992; p 9–121.

Table II. Fluorination of Nucleophiles by **1a**: Comparison between Predicted Dissociative Electron-Transfer Rate Constants and Experimental Rate Constants[a]

nu⁻	solvent (t, °C)	$E°_{\text{Nu•/Nu}}$[a] (V vs aq SCE)	λ_{Nu}[a] (eV)	k_{DET}[b] (M⁻¹ s⁻¹)	k_{exptl}[c] (M⁻¹ s⁻¹)
Me—C(CO₂Et)(CO₂Et) , K⁺	Et₂O (0)	0.34	2.60	5×10^{-15}	$\geq 8 \times 10^{-2}$
(2-methyl-3,4-dihydronaphthalen-1-olate) O⁻ , K⁺	THF (−78)	−0.4	2.17	3×10^{-15}	$\geq 3.2 \times 10^{-2}$
(1-naphthyl)Li	THF (−75)	−0.34	1.30	9×10^{-13}	1.9×10^{-2}

[a] From ref 2g. [b] Rate constant predicted for dissociative electron transfer. [c] Experimental rate constant.[2a]

withdrawing group is able to influence the electron density on the nitrogen atom.

Conclusions

One of the most important points to emerge from the preceding Results and Discussion is the experimental demonstration of the role of the bond dissociation energy, besides that of the height of the orbital possibly accommodating the incoming electron, in governing the passage between concerted and stepwise reductive cleavages. The weaker the bond, the more chance for the concerted mechanism to overrun the stepwise mechanism. Not only does this concept apply to the *N*-halosultams studied here, but it allows one to rationalize the observations previously made in an extended series of aryl, arylmethyl, and aliphatic halides. It should be emphasized that the conclusions thus drawn on electrochemical grounds are likewise applicable to homogeneous reactions with outer-sphere electron donors.

The observed effect of the bond dissociation energy on the passage from the concerted to the stepwise mechanism may be rationalized as follows, taking the peak potential E_p at a given scan rate as a measure of the electron free energy required to effect one or the other of the two reactions.

The standard potential for the dissociative electron transfer reaction (Z–X stands for the bond being broken, Z being a nitrogen atom, a carbon atom, or possibly another atom) is a function of the bond dissociation energy D_{ZX}, of the standard potential $E°_{X•/X⁻}$, and of an entropic term C' that does not vary much upon varying the substrate:

$$E°_{ZX/Z•+X⁻} = -D_{ZX} + E°_{X•/X⁻} + C' \qquad (12)$$

When one passes from one halogen to another as, for example, from **1a** to **1b** and **1c** or **2a** to **2b** and **2c**, D_{ZX} is not the only factor to change: $E°_{X•/X⁻}$ also varies, and it varies in the opposite direction. However, D_{ZX} (Table I) varies more rapidly than $E°_{X•/X⁻}$ (F, 2.62; Cl, 1.89; and Br, 1.48 V vs aqueous SCE). Thus, from a thermodynamic point of view, the dissociative electron-transfer reaction is more and more favorable when going from F to Cl and Br as expected intuitively. The intrinsic barrier $\Delta G^{\neq}_{0,ZX/Z•+X⁻}$ is, neglecting the relatively small variations of the solvent reorganization factor λ_0, essentially a function of the bond dissociation energy (eq 5). Dealing with general trends, it suffices to use the linearized version of the activation–driving force relationship (eq 11) as we have done to draw the straight line in Figure 5. Thus, when varying the leaving group:

$$(\Delta E_p)_{\text{concerted}} = -^3/_2 \Delta D_{ZX} + \Delta E°_{X•/X⁻} \qquad (13)$$

where the importance of the change in the bond dissociation energy

against that of $E°_{X•/X⁻}$ is enhanced by the variation of the intrinsic barrier.

In the stepwise case, the peak potential is a function of the cleavage rate constant of the anion radical that can be expressed, given the scan rate, as[10]

$$E_p = E°_{ZX/ZX•⁻} + \frac{RT}{2F} \ln k_c + \text{constant} \qquad (14)$$

with

$$\frac{RT}{F} \ln k_c = -\Delta G_c^{\neq} + \text{constant}$$

($-\Delta G_c^{\neq}$, cleavage activation free energy) as long as the cleavage of the anion radical is not too fast as compared to the electron transfer leading to its production. As shown elsewhere,[21] the cleavage activation free energy, $\Delta G^{\neq}_{ZX•⁻/Z•+X⁻}$, may also be expressed by a quadratic law:

$$\Delta G^{\neq}_{ZX•⁻/Z•+X⁻} = \Delta G^{\neq}_{0,\,ZX•⁻/Z•+X⁻} \left(1 + \frac{\Delta G°_{ZX•⁻/Z•+X⁻}}{4\Delta G^{\neq}_{0,\,ZX•⁻/Z•+X⁻}}\right)^2 \qquad (15)$$

where

$$\Delta G°_{ZX•⁻/Z•+X⁻} = D_{ZX} + E°_{ZX/ZX•⁻} - E°_{X•/X⁻} + \text{constant} \qquad (16)$$

and

$$\Delta G^{\neq}_{0,\,ZX•⁻/Z•+X⁻} = \frac{D_{ZX} + E°_{ZX/ZX•⁻} - E°_{Z•/(Z•)•⁻}}{4} \qquad (17)$$

It follows that upon changing the halogen:

$$(\Delta E_p)_{\text{stepwise}} = -^3/_8 \Delta D_{ZX} + ^1/_4 \Delta E°_{X•/X⁻} + ^5/_8 \Delta E°_{ZX/ZX•⁻} \qquad (18)$$

Thus, the stepwise reaction is favored, as is the concerted reaction, by a decrease of the factor $1.5 D_{ZX} - E°_{X•/X⁻}$. However, comparison between eqs 13 and 18 shows that the latter is much more favored than the former. It should be added that as $1.5 D_{ZX} - E°_{X•/X⁻}$ decreases, and therefore as the anion radical cleavage becomes faster and faster, the kinetic control of the stepwise reaction tend to pass to the forward outer-sphere electron transfer that produces the anion radical. This reaction is less sensitive to the variation of $1.5 D_{ZX} - E°_{X•/X⁻}$ than the cleavage of the anion radical, thus reinforcing the tendency for the concerted reaction to override the stepwise reaction.

(21) Savéant, J.-M., submitted for publication.

Control of Stepwise vs Concerted Reductive Cleavages

J. Am. Chem. Soc., Vol. 115, No. 15, 1993 6599

The above set of equations also allows one to understand the role of the π^* orbital energy, which varies as $-E^{\circ}_{ZX/ZX^{\bullet-}}$. The rate of the concerted reaction is insensitive to this factor, whereas a decrease of the π^* orbital energy strongly favors (eq 18) the stepwise reaction.

Another outcome of the present study is the determination of a series of *N*–halogen bond energies for which available data are scarce.

A last important result is the direct experimental determination of the standard potential of the $>N^{\bullet}/>N^-$ couple in aromatic sultams from the cyclic voltammetric oxidation of the corresponding amide ions. This parameter appears to be quite sensitive to substitution at the phenyl ring.

Experimental Section.

Chemicals. Acetonitrile (Merck Uvasol) was used as received, and DMF (Merck) was vacuum-distilled before use. The supporting electrolyte, *n*-Bu₄NBF₄ (Fluka, puriss), was used as received.

Sultams. 1a, 2a, 1d, and **2d** were prepared as previously described.[9b,d] The other sultams were prepared as follows. All solvents were analytical grade (Fluka) and used as received. Aliquat 336 ((tricaprylmethyl)ammonium chloride) was obtained from Aldrich; *tert*-butylhypochlorite[22] was obtained by a standard procedure. ¹H NMR spectra were recorded on a Bruker WM250 or a Varian XL300 with TMS as the internal standard. Chemical shifts are expressed in ppm versus TMS. Mass spectra, reported as *m/z* (relative intensity), were recorded on a Varian MAT 212. The reported melting points (°C) are uncorrected values.

1b. To an ice-cooled solution of 6.55 g (33 mmol, 1 equiv) of **1d** in 275 mL of methanol was added 6.6 g (61 mmol, 1.85 equiv) of *tert*-butylhypochlorite. The resulting mixture was stirred on ice for 2.5 h, then concentrated, dissolved in 250 mL of CHCl₃, washed with 50 mL of water, dried over magnesium sulfate, and evaporated to give 6.74 g of **1b** as white crystals (88%). mp: 88–89. ¹H-NMR (300 MHz, CDCl₃): 1.62 (s, 6H, 2CH₃), 7.47 (d, *J* = 7.5 Hz, 1H), 7.58 (t, *J* = 7.5 Hz, 1H), 7.72 (t, *J* = 7.5 Hz, 1H), 7.82 (d, *J* = 7.5 Hz, 1H). MS: 231/233 (10/3, M), 216/218 (100/38, M – CH₃), 182 (33, C₉H₁₀SO₂), 117 (25), 116 (14), 91 (15), 77 (10), 50 (10).

1c. To an ice-cooled solution of 5 g (25 mmol, 1 equiv) of **1d** in 30 mL of chloroform was added dropwise over a period of 30 min a solution of 8 g (50 mmol, 2 equiv) of bromine in 20 mL of NaOH (1 N). The flask was protected from light with an aluminium foil, and the mixture was stirred at O °C for an additional 3 h. The phases were separated, and the aqueous phase was washed with 50 mL of chloroform. The combined organic phases were washed with 50 mL of ice-cold water, dried over magnesium sulfate, and concentrated to give 2.8 g (57%) of **1c** as light yellow crystals. mp: 115–116. ¹H-NMR (250 MHz, CDCl₃): 1.60 (s, 6H, 2CH₃), 7.45 (d, *J* = 7.5 Hz, 1H), 7.53 (t, *J* = 7.5 Hz, 1H), 7.67 (t, *J* = 7.5 Hz, 1H), 7.83 (d, *J* = 7.5 Hz, 1H). MS: 275/277 (8/8, M), 260/262 (97/100, M – CH₃), 182 (94, C₉H₁₀SO₂), 117 (63), 91 (32), 77 (28), 50 (18).

1f. To a suspension of 3.6 g (65 mmol, 1.1 equiv) of powdered potassium hydroxide in 30 mL of THF was added dropwise a solution of 11.67 g (59.2 mmol, 1 equiv) of **1d**, 9.24 g (65.1 mmol, 1.1 equiv) of methyl iodide, and 2 drops of Aliquat 336. After the initial exothermal reaction, the white suspension was diluted with 30 mL of THF and refluxed for

2 h. Addition of water, extraction with methylene chloride, drying over magnesium sulfate, and concentration gave the crude product, which is purified by crystallization in ether/hexane to give 7.1 g (57%) of light yellow crystals. mp: 80–81. ¹H-NMR (250 MHz, CDCl₃): 1.54 (s, 6H, 2CH₃), 2.86 (s, 3H, CH₃), 7.43 (d, 7 Hz, 1H), 7.52 (t, *J* = 7 Hz, 1H), 7.64 (t, *J* = 7 Hz, 1H), 7.80 (d, *J* = 7 Hz, 1H). MS: 211 (5, M), 196 (100, M – CH₃), 117 (8), 91 (18), 56 (16).

2b. To an ice-cooled solution of 7.38 g (30.5 mmol, 1 equiv) of **2d** in 250 mL of methanol was added dropwise 5.3 g (49 mmol, 1.6 equiv) of *tert*-butylhypochlorite. After being stirring on ice for 3 h, the mixture was concentrated, dissolved in chloroform, and washed with water. Drying over magnesium sulfate and evaporation gave 7.8 g (93%) of pure **2b**. mp: 145–146. ¹H-NMR (250 MHz, CDCl₃): 1.70 (s, 6H, 2CH₃), 7.72 (d, *J* = 7.5 Hz, 1H), 8.58 (dd, *J* = 7.5 Hz, *J* = 1.2 Hz, 1H), 8.70 (d, *J* = 1.2 Hz, 1H). MS: 276/278 (6/3, M), 261/263 (100/40, M – CH₃), 227 (96, C₉H₁₀NO₄S), 215/217 (16/6, 261/263 – NO₂), 181 (30, 227 – NO₂), 116 (12), 75 (16).

2c. To a stirred suspension of 7.77 g (32 mmol, 1 equiv) of **2d** in 20 mL of NaOH (2 N) was added in 1 portion 6.4 g (40 mmol, 1.25 equiv) of bromine. The red-brown suspension which slowly turned yellow was filtered after 10 min, washed with ether, dried, and evaporated. Trituration in hot ether gave yellow crystals (9.9 g, 97%). mp: 168–169. ¹H-NMR (250 MHz, CD₃COCD₃): 1.80 (s, 6H, 2CH₃), 8.08 (d, *J* = 7.5 Hz, 1H), 8.75 (dd, *J* = 7.5 Hz, *J* = 1.5 Hz, 1H), 8.90 (d, *J* = 1.5 Hz, 1H). MS (CI, NH₃): 338/340 (25/25, M + 18), 260 (84), 230 (25), 215 (12), 213 (14), 197 (9), 180 (8), 137 (17), 136 (100), 134 (15), 118 (20), 110 (15), 108 (10).

2f. To a suspension of 3.64 g (65 mmol, 1.1 equiv) of powdered potassium hydroxyde in 30 mL of THF was added dropwise a solution of 14.34 g (59 mmol, 1 equiv) of **2d**, 9.23 mL (65 mmol, 1.1 equiv) of methyl iodide, and 2 drops of Aliquat 336 in 40 mL of THF. The initial exothermal reaction was kept at reflux for 2.5 h and then cooled to room temperature. Addition of water, extraction with methylene chloride, drying over magnesium sulfate, and concentration gave the crude product, which was recrystallized in methylene chloride/hexane to give light yellow crystals (11.2 g, 74%). mp: 160–161. ¹H-NMR (250 MHz, CDCl₃): 1.62 (s, 6H, 2CH₃), 2.92 (s, 3H, N–CH₃), 7.68 (d, 7.2 Hz, 1H), 8.53 (dd, *J* = 7.2 Hz, *J* = 1.5 Hz, 1H), 8.70 (d, *J* = 1.5 Hz, 1H). MS: 256 (6, M), 241 (100, M – CH₃), 211 (6, 241 – NO), 195 (66, 241 – NO₂), 130 (7), 90 (10), 89 (10), 56 (19).

Instrumentation. Most of the cyclic voltammetric experiments were carried out with a 3-mm-diameter glassy carbon disk. At the highest scan rates investigated with this electrode material (100–1500 V/s), a 0.25-mm disk was used. In the high-scan-rate experiments we used a 10-μm-diameter carbon disk (Princetown Applied Research). The electrodes were carefully polished and ultrasonically rinsed with ethanol before each run. The counter electrode was a platinum wire and the reference electrode an aqueous SCE electrode. A graphite crucible was used as the anode in the preparative-scale oxidation of **1e**, and the resulting dimer was identified by its mass peak. An acetonitrile solution of **1e** (50 mL), obtained from the deprotonation of **1d** (0.05 M) by (CH₃)₄NOH (0.04 M), was electrolyzed at 0.85 V vs SCE. After the passage of 190 C (1e/molecule), the solution was acidified by a 0.1 M HCl solution. After ether extraction, evaporation, and recrystallization in ethanol, a compound with the following mass spectrum was obtained. MS (CI, NH₃): 410 (74, M + 18)

The potentiostat, equipped with a positive feedback compensation and current measurer, used at low or moderate scan rates, was the same as previously described.[22a] The instrument used with ultramicroelectrodes at high scan rates has been described elsewhere.[22b]

(22) Teetrer, H. M.; Bell, E. W. *Org. Synth. Collect.* **1963**, *4*, 125.

(23) (a) Garreau, D.; Savéant, J.-M. *J. Electroanal. Chem.* **1972**, *35*, 309. (b) Garreau, D.; Hapiot, P.; Savéant, J.-M. *J. Electroanal. Chem.* **1989**, *272*, 1.